JOURNAL OF INDUSTRIAL AND MANAGEMENT OPTIMIZATION
Volume **5**, Number **2**, May **2009**
doi:10.3934/jimo.2009.5.xx
pp. **1–XX**

EXTENSIONS OF INCOMPLETE OBLIQUE PROJECTIONS METHOD FOR SOLVING RANK-DEFICIENT LEAST-SQUARES PROBLEMS

H. D. Scolnik

Dto. de Computación, Fac. de Ciencias Exactas y Naturales. UBA
Pabellón 1, Ciudad Universitaria
Buenos Aires, C1428EGA, Argentina

N. E. Echebest

Departamento de Matemática, Fac. de Ciencias Exactas. UNLP
P.O. Box 172. La Plata,1900, Argentina

M. T. Guardarucci

Departamento de C. Básicas, Fac. de Ingeniería. UNLP
La Plata, 1900, Argentina

Abstract. The aim of this paper is to extend the applicability of an algorithm for solving inconsistent linear systems to the rank-deficient case, by employing incomplete projections onto the set of solutions of the augmented system $Ax - r = b$. The extended algorithm converges to the unique minimal norm solution of the least squares solutions. For that purpose, incomplete oblique projections are used, defined by means of matrices that penalize the norm of the residuals. The theoretical properties of the new algorithm are analyzed, and numerical experiences are presented comparing its performance with some well-known projection methods.

1. **Introduction.** Large and sparse systems of linear equations arise in many important applications [9, 14], as image reconstruction from projections, radiation therapy treatments planning, and other image processing problems as electromagnetic geotomography [20], computational mechanics, optimization, etc. In practice, those systems are often inconsistent, and one usually seeks a point $x^* \in \Re^n$ that minimizes a certain proximity function. A common approach to such problems is to use algorithms, see for instance Y. Censor and S. Zenios [6] and [1], which employ projections onto convex sets in various ways, using either sequential or simultaneous projections onto the hyperplanes represented by the rows of the complete system or onto blocks of a given partition. A widely used algorithm in Computerized Tomography is ART (Algebraic Reconstruction Technique), whose origin goes back to Kaczmarz [16], although it is known that in order to get convergence it is necessary to use an underrelaxation parameter that must tend to zero. C. Popa [19]

2000 *Mathematics Subject Classification.* Primary: 90C25; Secondary: 90C30.
Key words and phrases. Rank-deficient least-squares problems, minimal norm solution, incomplete oblique projections.
Work supported by the universities of Buenos Aires and La Plata (Project 11/X473), Argentina.

extended their algorithm (KERP) for getting convergence in the inconsistent case. More recently, in [20] the authors showed the efficiency of the KERP algorithm for solving rank deficient systems. For the classical simultaneous projection algorithms for inconsistent problems, as Cimmino, SART [6], Landweber [18], CAV [7] and the more general class of the diagonal weighting algorithms(DWE) [8], in order to prove convergence in the inconsistent case it is necessary to choose the relaxation parameter in an interval that depends on the largest eigenvalue of A^TA [3, 17]. Within the framework of the Projected Aggregation Methods (PAM) [15, 13] we have developed acceleration schemes [12, 21, 22] based on projecting the search directions onto the aggregated hyperplanes, with excellent results for consistent problems. We also extended these ideas in [23] for inconsistent problems introducing the IOP algorithm that converges to a weighted least squares solution of the system $Ax = b$. In this paper, we adapted the above mentioned IOP algorithm in order to compute the weighted least squares solution of inconsistent and rank-deficient systems. This algorithm uses an incomplete oblique projections scheme onto the solution set of the augmented system $Ax - r = b$. More explicitly, in order to solve a possibly inconsistent system $Ax = b$, $A \in \Re^{m\times n}$, $b \in \Re^m$, we consider the standard problem:

$$\min_{x\in\Re^n} \|b - Ax\|^2_{D_m}, \tag{1}$$

where $\|.\|_{D_m}$ denotes the norm induced by the positive definite diagonal matrix $D_m \in \Re^{m\times m}$, whose solutions coincide with those of the problem

$$A^TD_mAx = A^TD_mb. \tag{2}$$

In [23] we proved that is equivalent to the problem

$$\min\{\|p - q\|^2_D : \quad \text{for all } \ p \in \mathcal{P} \text{ and } \quad q \in \mathcal{Q}\}, \tag{3}$$

$\mathcal{P}$ and $\mathcal{Q}$ being two convex sets in the $(n + m)$-dimensional space $\Re^{n+m}$, such that denoting by $[u; v]$ the vertical concatenation of $u \in \Re^n$, with $v \in \Re^m$,

$$\mathcal{P} = \{p : p = [x; r] \in \Re^{n+m}, \quad x \in \Re^n, \quad r \in \Re^m, \quad Ax - r = b\}, \text{ and} \tag{4}$$

$$\mathcal{Q} = \{q : q = [x; 0] \in \Re^{n+m}, \quad x \in \Re^n, 0 \in \Re^m\}, \tag{5}$$

adopting the distance $d(p, q) = \|p - q\|_D$, for all $p \in \mathcal{P}$, $q \in \mathcal{Q}$. D is a diagonal matrix of order $n + m$, whose n first elements are 1's, and the last m coincide with those of D_m. By means of a direct application of the Karush-Kuhn-Tucker(KKT) [6] conditions we obtain that its solutions $p^* \in \mathcal{P}$, $p^* = [x^*; r^*]$, and $q^* = [y^*; 0] \in \mathcal{Q}$, satisfy $x^* = y^*$, $A^TD_mr^* = 0$, and $\|p^* - q^*\|^2_D = \|r^*\|^2_{D_m}$. That result led us to develop the IOP method for solving (1), applying an alternate projections scheme between the sets $\mathcal{P}$ and $\mathcal{Q}$, similar to the one of Csiszár and Tusnády [10], but replacing the computation of the exact projections onto $\mathcal{P}$ by suitable incomplete or approximate projections, according to the following basic scheme:

Algorithm 1. (Basic Alternating Scheme)
Iterative step: *Given* $p^k = [x^k; r^k] \in \mathcal{P}$, $q^k = [x^k; 0] \in \mathcal{Q}$,
find $p^{k+1}_a = [x^{k+1}; r^{k+1}] \in \mathcal{P}$ as:

$$p^{k+1}_a \approx \arg\min\{\|p - q^k\|^2_D : p \in \mathcal{P}\}, \quad \text{then}$$

define $p^{k+1} = p^{k+1}_a$, *and* $q^{k+1} \in \mathcal{Q}$ by means of

$$q^{k+1} = [x^{k+1}; 0] \equiv \arg\min\{\|p^{k+1} - q\|^2_D : \quad q \in \mathcal{Q}\}.$$

In order to compute the incomplete projections onto $\mathcal{P}$ we apply our ACCIM algorithm [22, 23]. Aiming at clarifying the applicability of ACCIM within the new approach, it is convenient to point out that, given a consistent system, $\bar{A}y = \bar{b}$, the sequence $\{y^k\}$ generated by ACCIM, from the initial point y^0, converges to the solution $\bar{y}^*$ of $\bar{A}y = \bar{b}$, satisfying

$$\bar{y}^* = \arg\min\{\|y^* - y^0\|_D^2, \quad y^* \in \Re^n : \bar{A}y^* = \bar{b}\}. \tag{6}$$

This iterative algorithm uses simultaneous projections onto the hyperplanes defined by the rows of $Ax - r = b$, and is very efficient for solving consistent problems and convenient for computing approximate projections with some required properties, as explained in [23].

In the following sections we will present the EIOP algorithm based on the same basic scheme of Algorithm 1, but adding more restrictive conditions for accepting an approximate solution in $\mathcal{P}$ for the special case of rank deficient problems.

We report numerical experiences for comparing the performance of the new algorithm with those of Landweber(LANDW) [18] and Kaczmarz Extended(KERP) [19]. We also consider simulations of image reconstruction problems with limited data, as those arising in electromagnetic geotomography [20] that lead to rank deficient inconsistent problems, usually very ill-conditioned.

The paper is organized as follows: In Section 2 we briefly review some notation and results necessary for describing the new algorithm. In section 3 the new oblique projection *EIOP* algorithm is presented together with some related results needed for defining it and the corresponding convergence theory. In Section 5 numerical experiences are described, together with some preliminary conclusions.

2. **Projections algorithms.** From hereafter $\|x\|$ will denote the *Euclidean* norm of $x \in \Re^n$, and $\|x\|_D$ the norm induced by a positive definite matrix D. We will also assume that each row of A has an *Euclidean* norm equal to 1.

We will use the notation $\mathbf{e}_i$ for the i-th column of I_n, where the symbol I_n denotes the identity matrix in $\Re^{n\times n}$, and the upper index T for the transpose of a matrix. Given $M \in \Re^{n\times r}$ we will denote by $\mathbf{m}_i^T$ the i-th row of M, and by $R(M)$ the subspace spanned by the columns of M, P_M and P_M^D the orthogonal and the oblique projectors onto $R(M)$. We will use the notation $R(M)^\perp$ for the D-orthogonal subspace to $R(M)$, and by $P_{M^\perp}^D$ the corresponding projector. In particular, if $M = [v] \in \Re^{n\times 1}$, we will use $P_{v^\perp}^D$. We denote a diagonal matrix of order n, by $D = diag(d)$, where $d = (d_1, \ldots, d_n)$.

Let us assume we have a compatible system $\bar{A}y = \bar{b}$, $\bar{A} \in \Re^{m\times n}$, $m \geq n$, $\bar{b} \in \Re^m$.

For each constraint of $\bar{A}y = \bar{b}$, we will denote by $L_i = \{y \in \Re^n : \bar{\mathbf{a}}_i^T y = b_i\}$, $r_i(y) = \bar{\mathbf{a}}_i^T y - b_i$, and the oblique projection of y onto L_i by

$$P_i^D(y) = y - \frac{r_i(y)}{\bar{\mathbf{a}}_i^T D^{-1} \bar{\mathbf{a}}_i} D^{-1} \bar{\mathbf{a}}_i. \tag{7}$$

3. **Inconsistent case.** As said in the Introduction, for possibly inconsistent systems $Ax = b$, $A \in \Re^{m\times n}$, $b \in \Re^m$, $m \geq n$, we will consider the standard problem (1), whose solution coincides with the one of the problem:

$$A^T D_m A x = A^T D_m b.$$

In [23] we had presented algorithms that are particular cases of the Algorithm 1, together with the convergence results for the case $rank(A) = n$. In the following,

we extend those results in order to compute the weighted least squares solution of inconsistent and rank-deficient systems.

3.1. **Incomplete oblique projections algorithm.** We consider a diagonal weighting matrix $D \in \Re^{n+m \times n+m}$,

$$D = \begin{pmatrix} I_n & 0 \\ 0 & D_m \end{pmatrix}, \tag{8}$$

and the sets $\mathcal{P}$ and $\mathcal{Q}$ as described in (4) and (5).

Given $p^k \in \mathcal{P}$, and its projection q^k onto $\mathcal{Q}$, we will denote by $p^D_{min}(q^k)$ the projection of q^k onto $\mathcal{P}$, which is the solution of the problem

$$\min\{\|p - q^k\|_D : \quad p \in \mathcal{P}\}. \tag{9}$$

In particular, if $p^* = [x^*; r^*] \in \mathcal{P}$, with x^* solution of (1), and its projection onto $\mathcal{Q}$, $q^* = [x^*; 0]$, we get $p^* = p^D_{min}(q^*)$, and the minimum distance between the sets $\mathcal{P}$ and $\mathcal{Q}$ is $\|r^*\|^2_{D_m}$.

In the new algorithm, given $q^k \in \mathcal{Q}$ instead of defining $p^{k+1} = p^D_{min}(q^k)$, we define $p^{k+1} = p^{k+1}_a$, where $p^{k+1}_a \in \mathcal{P}$ is a point obtained by means of the incomplete resolution of the problem (9).

Remark 1. The results in [4] allow us to prove the sequence given by the Algorithm 1 is convergent when $p^{k+1} = p^D_{min}(q^k)$.

As mentioned before, the algorithm based on exact projections is always convergent, but its computational cost is high. Therefore, we have presented in [23] the theory of inexact projections aiming at getting similar convergence properties but with a much lower computational cost.

In order to define the inexact projection $p^{k+1}_a \approx p^D_{min}(q^k)$, we consider the following:

Definition 3.1. Given an approximation $\hat{p} = [z; \mu]$, $z \in \Re^n$, $\mu \in \Re^m$, of $p^D_{min}(q^k)$, we will denote by $P(\hat{p}) = [z; \mu + s]$, the solution of the system $Ax - r = b$ that satisfies $\mu + s = Az - b$.

Aiming at obtaining properties of the sequence $\{p^k\}$ generated by the new algorithm that guarantees convergence to the solution of (3) we establish an "acceptance condition" that an approximation $\hat{p} = [z; \mu]$ of $p^D_{min}(q^k)$ must satisfy.

Definition 3.2. Acceptance Condition. An approximation $\hat{p} = [z; \mu]$ of $p^D_{min}(q^k)$ is acceptable if it satisfies that $\|\hat{p} - q^k\|^2_D \leq \|p^D_{min}(q^k) - q^k\|^2_D$ and

$$\|\hat{p} - P(\hat{p})\|^2_D \leq \gamma \|\hat{p} - p^k\|^2_D, \quad \text{with} \quad 0 < \gamma < 1. \tag{10}$$

In order to describe the alternate incomplete projections algorithm, we define the approximation p^{k+1}_a of $p^D_{min}(q^k)$, by

Definition 3.3.

$$p^{k+1}_a = P(\hat{p}), \quad \text{if} \quad \hat{p} = [z^j; \mu^j] \quad \text{satisfies} \quad (10). \tag{11}$$

Remark 2. In particular, $\hat{p} = p^D_{min}(q^k)$ satisfies (10).

We have proved in Lemma 1 in [23] that using the ACCIM Algorithm, it is possible to find a $j > 0$, such that $[z^j; \mu^j]$ satisfies (10). An oblique version of ACCIM [22] algorithm for solving consistent problems is described in [23].

We present in the following a practical algorithm to solve (1):

Algorithm 2. Extension of Incomplete Oblique Projections (EIOP)
Initialization: Given $0 < \gamma \leq 1/2$, a positive definite diagonal matrix D_m of order m and $p^0 = [x^0; r^0]$, set $r^0 = Ax^0 - b$, $q^0 = [x^0; 0] \in \mathcal{Q}$ and $k \leftarrow 0$.
Iterative Step: *Given* $p^k = [x^k; r^k]$, *set* $q^k = [x^k; 0]$.

- *Calculate* $\hat{p}$, *approximation of* $p^D_{min}(q^k)$ *satisfying (10), applying ACCIM as follows: Define* $y^0 = [z^0; \mu^0] = q^k$ *the initial point.*
  For solving $Ax - r = b$, *iterate until finding* $y^j = [z^j; \mu^j]$, *such that* $s^j = Az^j - \mu^j - b$ *satisfies (10), that is*

$$\|s^j\|^2_{D_m} \leq \gamma(\|r^k\|^2_{D_m} - \mathcal{S}_j), \text{ with } \mathcal{S}_j = \|y^j - y^0\|^2_D. \tag{12}$$

- Define $p^{k+1} = [x^{k+1}; r^{k+1}]$, *being* $x^{k+1} = z^j$, *and* $r^{k+1} = \mu^j + s^j$.
- Define $q^{k+1} = [x^{k+1}; 0] \in \mathcal{Q}$.
- $k \leftarrow k + 1$.

3.2. **Convergence of the EIOP algorithm.** We will consider the following sets:

$$L^{D_m}_{sq} = \{x^* \in \Re^n : \text{ for which } r^* = Ax^* - b \text{ satisfies } A^T D_m r^* = 0\}, \tag{13}$$

the set of solutions to the problem (1), and the corresponding

$$\mathcal{S}^{D_m} = \{p^* : p^* = [x^*; r^*] \in \mathcal{P} \text{ such that } x^* \in L^{D_m}_{sq}\}. \tag{14}$$

We will prove that the sequence given by Algorithm 2 converges to an element of the set $\mathcal{S}^{D_m}$, with D_m the matrix arising from (8).

Given an initial point $q^0 = [x^0; 0] \in \mathcal{Q}$, we consider

$$\bar{x^*} = \arg \min_{x^* \in L^{D_m}_{sq}} \|x^0 - x^*\|^2 \tag{15}$$

and $\bar{p^*} = [\bar{x^*}; r^*] \in \mathcal{S}^{D_m}$, which satisfies

$$\bar{p^*} = \arg \min_{p^* \in \mathcal{S}^{D_m}} \|q^0 - p^*\|^2_D, \tag{16}$$

because $\|q^0 - p^*\|^2_D = \|x^0 - x^*\|^2 + \|r^*\|^2_{D_m}$.

Aiming at proving that the sequence $\{p^k\}$ generated by the new version of IOP algorithm is convergent, we will study the relationship between two consecutive iterates p^k and p^{k+1}.

Lemma 3.4. *Let* $\{p^k\} = \{[x^k; r^k]\}$ *be the sequence generated by the Algorithm 2, then*
(i) $p^k = [x^k; r^k]$ *and* $p^{k+1} = [x^{k+1}; r^{k+1}]$ *satisfy*
$\|r^{k+1}\|^2_{D_m} \leq \|r^k\|^2_{D_m} - (1 - \gamma)\|p^k - p^D_{min}(q^k)\|^2_D$.
(ii) The sequence $\{\|r^k\|_{D_m}\}$ *is decreasing and bounded, therefore it converges.*
(iii) The following three sequences tend to zero: $\{\|p^k - p^D_{min}(q^k)\|^2_D\}$, $\{\|p^{k+1} - p^D_{min}(q^k)\|^2_D\}$, *and* $\{\|p^{k+1} - p^k\|^2_D\}$.
(iv) The sequence $\{\|A^T D_m r^k\|\}$ *goes to zero.*
(v) If $\bar{x^*} = \arg\min_{x^* \in L^{D_m}_{sq}} \|x^* - x^k\|^2$, *then* $\bar{x^*}$ *also fulfills that property in regard to* x^{k+1}.

Proof. The proof is similar to the one of Lemma 3 in [23]. □

The hypothesis on the parameter γ is restricted to $0 < \gamma \leq 1/2$. This will allow us to extend the result of the Lemma 4 in [23] to problems with $rank(A) < n$.

Theorem 3.5. *Let $\{p^k\}$ be the sequence generated by the Algorithm 2, using $0 < \gamma \leq 1/2$. If $\bar{p^*} = [\bar{x^*}; r^*]$ is the element defined in (16), and its projection $\bar{q^*} = [\bar{x^*}; 0] \in \mathcal{Q}$, then*
(i) the sequence $\{\|p^k - \bar{q^*}\|_D^2\}$ is decreasing and bounded, hence it converges.
(ii) The sequence $\{p^k\}$ converges to $\bar{p^*}$.

4. **Proofs.** With the purpose of analyzing this algorithm's behavior, we need to describe some properties related to the inner iterative steps arising from the use of ACCIM, which is the basis for computing approximate solutions to the problem (9) in the EIOP algorithm.

4.1. **Applying ACCIM to solve Ax -r = b.** Assume that $\bar{A}y = \bar{b}$, is a consistent system where $\bar{A} \in \Re^{m \times n}$, and y^* a solution to it. Let $\{y^j\}$ be the sequence generated by a version of the ACCIM algorithm with a D-norm, and $s^j = \bar{A}y^j - \bar{b}$ the residual at each iterate y^j.
The direction d^j defined in ACCIM (see Appendix A in [23]) by combining the projections (7) is

$$d^j = \sum_{l=1}^{m} w_l (P_l^D(y^j) - y^j) = -\sum_{l=1}^{m} w_l \frac{s_l^j}{\|\bar{a}_l\|_{D^{-1}}^2} D^{-1} \bar{a}_l. \tag{17}$$

At each iterate $y^j \neq y^*$, $j > 0$, the direction used is $\hat{d^j} = P_{v^\perp}(d^j)$, where $v = \hat{d^{j-1}}$, and the next iterate $y^{j+1} = y^j + \lambda_j \hat{d^j}$, satisfies

$$(\hat{d^j})^T D(y^j - y^* + \lambda_j \hat{d^j}) = 0. \tag{18}$$

Furthermore, from the definition of $\hat{d^j}$ and λ_j, it is possible to obtain:

Lemma 4.1. *If $y^j \neq y^*$, $j > 0$, is generated by the ACCIM algorithm, then*
(i) d^j is D-orthogonal to $y^* - y^i$, for all $i < j$.
(ii) $\hat{d^j}$ is D-orthogonal to $\hat{d^i}$ and d^i, for all $i < j$.
Furthermore,
(iii) $y^* - y^j$ is D-orthogonal to $\hat{d^i}$, for all $i < j$, and as a consequence is also D-orthogonal to $y^j - y^0$.

Proof. See the proof of Lemma 2, Appendix A, in [23]. □

In particular, the application of ACCIM for solving $Az - I_m r = b$ has the following characteristics:
Given p^k and $q^k = [x^k; 0]$, $k \geq 0$, ACCIM computes an approximation $[z^j; \mu^j]$ to the projection $p_{min}^D(q^k)$.

In order to solve (9), from the starting point $[z^0; \mu^0] = q^k = [x^k; 0]$, for each iterate $[z^j; \mu^j]$, we denote by s^j the residual $s^j = Az^j - \mu^j - b$. The direction $d^j \in \Re^{n+m}$, can be written as

$$d^j = -\sum_{i=1}^{m} w_i \frac{s_i^j}{\|\bar{\mathbf{a}}_i\|_{D^{-1}}^2} (D)^{-1} \bar{\mathbf{a}}_i, \tag{19}$$

$\bar{\mathbf{a}}_i = [\mathbf{a}_i; -\mathbf{e}_i]$ being the i-th column of $[A, -I_m]^T$, where $\mathbf{e}_i$ denotes the i-th column of I_m. The square of the norm of each row of the matrix $[A, -I_m]$, induced by the inverse of D, is $1 + 1/(D_m)_i$, if $\|\mathbf{a}_i\| = 1$ and $(D_m)_i$ denotes the i-th element of

the diagonal of D_m. Hence, the direction $d^j = [d_1^j; d_2^j]$ has its first n components given by:

$$d_1^j = -\sum_{i=1}^{m} \frac{w_i (D_m)_i s_i^j}{1 + (D_m)_i} \mathbf{a}_i \tag{20}$$

and the next m-components are

$$d_2^j = (D_m)^{-1} \sum_{i=1}^{m} \frac{w_i (D_m)_i s_i^j}{1 + (D_m)_i} \mathbf{e}_i. \tag{21}$$

We choose for this application of ACCIM the values w_i : $w_i = 1 + (D_m)_i$, because they privilege the rows with greatest $1 + (D_m)_i$. Thus, at each iterate $[z^j; \mu^j]$, the directions are:

$$d_1^j = -\sum_{i=1}^{m} (D_m)_i \mathbf{a}_i s_i^j = A^T D_m(-s^j), \quad \text{and} \quad d_2^j = \sum_{i=1}^{m} \mathbf{e}_i s_i^j = s^j. \tag{22}$$

This direction d^j is such that $d_1^j = A^T D_m(-d_2^j)$. Similar behavior has the direction $\hat{d}^j = [\hat{d}_1^j; \hat{d}_2^j]$, where $\hat{d}_1^j = A^T D_m(-\hat{d}_2^j)$; expression that follows from considering $\hat{d}_1^j = d_1^j - \frac{(\hat{d}^{j-1})^T D d^j}{\|\hat{d}^{j-1}\|_D^2} \hat{d}_1^{j-1}$, and $\hat{d}_2^j = d_2^j - \frac{(\hat{d}^{j-1})^T D d^j}{\|\hat{d}^{j-1}\|_D^2} \hat{d}_2^{j-1}$, and using that $\hat{d}^0$ coincides with d^0. Hence, for each $j > 0$, $[z^j; \mu^j]$ satisfies $z^j - z^0 = A^T D_m(-\mu^j)$.

Remark 3. We will describe now the properties of the accepted approximation $\hat{p} = [z^j; \mu^j]$, in the iterations of the Algorithm 2.

(a) From (iii) of the previous Lemma, we know that for every solution $[z^*; \mu^*]$ of $Az - \mu = b$, $[z^*; \mu^*] - [z_j; \mu_j]$ is D-orthogonal to $[z_j; \mu_j] - [z_0, \mu_0]$. Thus, for all $p \in \mathcal{P}$, we have that

$$(p - \hat{p})^T D(\hat{p} - q^k) = 0. \tag{23}$$

(b) From (i) of the previous Lemma we know that for every $[z^j; \mu^j]$, $j > 0$, the direction d^j satisfies ${d^j}^T D([z^*; \mu^*] - [z^0; \mu^0]) = 0$. Then, since $p^k \in \mathcal{P}$ and $q^k = [z^0; \mu^0]$, in particular ${d^j}^T D(p^k - q^k) = 0$. Hence, using the expression of d^j in (22), and considering that $p^k - q^k = [0; r^k]$, we get that

$$s^j \quad \text{is } D_m\text{-orthogonal to} \quad r^k. \tag{24}$$

(c) Furthermore, considering (a) and (b) it follows that $p^k - \hat{p}$ is D-orthogonal to $[0; s^j]$.

Remark 4. The inequality (12), used in Algorithm 2 to accept $[z^j; \mu^j]$, arises from replacing in the inequality of (10), $\|\hat{p} - P(\hat{p})\|_D^2 = \|s^j\|_{D_m}^2$, and $\|p^k - \hat{p}\|_D^2 = \|(p^k - q^k) - (\hat{p} - q^k)\|^2$. Moreover, from (23) we know that $p^k - \hat{p}$ and $\hat{p} - q^k$ are D-orthogonal, and using the fact that $\|p^k - q^k\|_D^2 = \|[0; r^k]\|_D^2 = \|r^k\|_{D_m}^2$, we get that $\|p^k - \hat{p}\|_D^2 = \|r^k\|_{D_m}^2 - \|\hat{p} - q^k\|_D^2$. Also, using again the results of Lemma 4.1, we get $\|\hat{p} - q^k\|_D^2 = \|y^j - y^0\|_D^2$.

4.2. **Proof of Theorem 3.5.**

Proof. To prove (i), let us consider the computation of the distance $\|p^k - \bar{q^*}\|_D^2$ and $\|p^{k+1} - \bar{q^*}\|_D^2$. The first, $\|p^k - \bar{q^*}\|_D^2$, using the intermediate point $q^{k+1} = [x^{k+1}; 0]$, coincides with $\|p^k - \bar{q^*}\|_D^2 = \|p^k - q^{k+1}\|_D^2 + \|q^{k+1} - \bar{q^*}\|_D^2 + 2(q^{k+1} - p^k)^T D(\bar{q^*} - q^{k+1})$. Using the coordinates of the points represented by p^k, q^{k+1} and $\bar{q^*}$, we get that $\|p^k - \bar{q^*}\|_D^2 = \|r^k\|_{D_m}^2 + \|x^{k+1} - x^k\|^2 + \|x^{k+1} - \bar{x^*}\|^2 + 2(x^{k+1} - x^k)^T(\bar{x^*} - x^{k+1})$.

Since $p^{k+1} = [x^{k+1}; r^{k+1}]$ it follows from the approximation $\hat{p} = [z^j; \mu^j]$ satisfying the condition (11), we know that $x^{k+1} = z^j$, $r^{k+1} = \mu^j + s^j$, where $s^j = Ax^{k+1} - \mu^j - b$. Furthermore, as a consequence of the iterative process of ACCIM we also know, according to the results in subsection 4.1, that $x^{k+1} - x^k = A^T D_m(-\mu^j)$. Then, $(x^{k+1} - x^k)^T(\bar{x^*} - x^{k+1}) = -{\mu^j}^T D_m(r^* - r^{k+1})$.
Taking into account the ACCIM properties (i)(ii) and (iii) of Lemma 4.1, and its specific application in Remark 3 to the problem solved by Algorithm 2, we get that $-{\mu^j}^T D_m(r^* - r^{k+1}) = -{\mu^j}^T D_m r^* + \|\mu^j\|^2_{D_m}$. Hence, $\|p^k - \bar{q^*}\|^2_D$ is equal to $\|r^k\|^2_{D_m} + \|x^{k+1} - x^k\|^2 + \|x^{k+1} - \bar{x^*}\|^2 + 2\|\mu^j\|^2_{D_m} - 2\mu^j D_m r^*$.

Let us consider now $\|p^{k+1} - \bar{q^*}\|^2_D = \|x^{k+1} - \bar{x^*}\|^2 + \|r^{k+1}\|^2_{D_m}$. Due to (b) of the Remark 3 we know that ${s^j}^T D_m \mu^j = 0$, and $\|r^{k+1}\|^2_{D_m} = \|s_j\|^2_{D_m} + \|\mu^j\|^2_{D_m}$. Hence, the difference $\|p^k - \bar{q^*}\|^2_D - \|p^{k+1} - \bar{q^*}\|^2_D$, can be described by means $\|r^k\|^2_{D_m} + \|x^{k+1} - x^k\|^2 + (\|\mu^j\|^2_{D_m} - 2{\mu^j}^T D_m r^* + \|r^*\|^2_{D_m}) - \|r^*\|^2_{D_m} - \|s^j\|^2_{D_m}$, after having added and subtracted $\|r^*\|^2_{D_m}$. Then, considering that $\|\mu^j\|^2_{D_m} - 2{\mu^j}^T D_m r^* + \|r^*\|^2_{D_m} = \|\mu^j - r^*\|^2_{D_m} \geq 0$, we get that $\|p^k - \bar{q^*}\|^2_D - \|p^{k+1} - \bar{q^*}\|^2_D \geq \|r^k\|^2_{D_m} + \|x^{k+1} - x^k\|^2 - \|s^j\|^2_{D_m} - \|r^*\|^2_{D_m}$.

On the other hand, from (a) of Remark 3 we know that $\|r^k\|^2_{D_m} = \|q^k - \hat{p}\|^2_D + \|p^k - \hat{p}\|^2_D$. Also, it is known by the acceptability condition (10) that $\|s^j\|^2_{D_m} \leq \gamma\|p^k - \hat{p}\|^2_D$, with $0 < \gamma \leq 1/2$. Then, the difference $\|p^k - \bar{q^*}\|^2_D - \|p^{k+1} - \bar{q^*}\|^2_D \geq \|q^k - \hat{p}\|^2_D + (\frac{1}{\gamma} - 1)\|s^j\|^2_{D_m} - \|r^*\|^2_{D_m}$. Furthermore, considering that $\|q^k - \hat{p}\|^2_D = \|x^{k+1} - x^k\|^2 + \|\mu^j\|^2_{D_m}$, by hypothesis $(\frac{1}{\gamma} - 1)\|s^j\|^2_{D_m} \geq \|s^j\|^2_{D_m}$, and $\|r^{k+1}\|^2_{D_m} = \|\mu^j\|^2_{D_m} + \|s^j\|^2_{D_m}$, we get that the difference $\|p^k - \bar{q^*}\|^2_D - \|p^{k+1} - \bar{q^*}\|^2_D \geq \|r^{k+1}\|^2_{D_m} - \|r^*\|^2_{D_m}$. Therefore, the sequence $\{\|p^k - \bar{q^*}\|^2_D\}$ is decreasing, bounded, and therefore convergent.

Since we know that the sequence $\{\|p^k - \bar{q^*}\|^2_D\}$ converges, we get a similar result for the sequence $\{\|p^k - \bar{p^*}\|^2_D\}$ considering that $\|p^k - \bar{p^*}\|^2_D = \|(p^k - \bar{q^*}) - (\bar{p^*} - \bar{q^*})\|^2_D$. Using the orthogonality between $p^k - \bar{p^*}$ and $\bar{p^*} - \bar{q^*}$, and considering that $\bar{p^*} - \bar{q^*} = [0; r^*]$, we get $\|p^k - \bar{p^*}\|^2_D = \|(p^k - \bar{q^*})\|^2_D - \|r^*\|^2_{D_m}$. Therefore, since the sequence $\{\|p^k - \bar{q^*}\|^2_D\}$ is decreasing and convergent, the sequence $\|p^k - \bar{p^*}\|^2_D$ also converges.

From the fact the distances $\{\|p^k - \bar{p^*}\|^2_D\}$ decrease, $\bar{p^*}$ being the element defined in (16), it follows that the sequence $\{p^k\}$ is in a compact set $\mathcal{B}_0$, centered in $\bar{p^*}$, because it satisfies $\|p^k - \bar{p^*}\|^2_D < \|p^0 - \bar{p^*}\|^2_D$. Hence, a subsequence $\{p^{k_s}\} = \{[x^{k_s}; r^{k_s}]\}$ exists, satisfying $r^{k_s} = Ax^{k_s} - b$, convergent to $[\overline{x}; \overline{r}] \in \mathcal{B}_0$.

By (iv) of the Lemma 3.4, we know that $A^T D_m r^{k_s}$ tends to zero, then $A^T D_m \overline{r} = 0$. Therefore, $[\overline{x}; \overline{r}]$ satisfies the optimality condition of the problem (1). Moreover, $\overline{r} = r^*$ because of the unicity of the minimal residual r^*.

Furthermore, since $\|\overline{x} - \bar{x^*}\| \leq \|x^{k_s} - \overline{x}\| + \|x^{k_s} - \bar{x^*}\|$, due to (v) of the Lemma 3.4 we know that $\|x^{k_s} - \bar{x^*}\| \leq \|x^{k_s} - \overline{x}\|$, therefore $\|\overline{x} - \bar{x^*}\| \leq 2\|x^{k_s} - \overline{x}\|$. Hence, we get that $\overline{x} = \bar{x^*}$.

Finally, since the sequence of the norms $\|p^k - \bar{p^*}\|_D$ converges, and the subsequence $\|p^{k_s} - \bar{p^*}\|_D$ goes to zero, the sequence $\|p^k - \bar{p^*}\|_D$ tends to zero. Therefore, the sequence $\{p^k\}$ converges to $\bar{p^*}$. □

5. **Numerical experiments.** The objectives of the following experiences are two-fold. First we compare our algorithm with other methods, in relation to the rate of decrease of the norm of the residual, also reporting the number of iterations needed for satisfying the convergence conditions and the corresponding CPU time. In the

second part we analyze the EIOP's behavior when solving image reconstruction problems. All visualizations have been obtained using MATLAB 5.3.

For the first purpose, we made some comparisons of the algorithms EIOP, KERP [20] using the relaxation parameters values the authors reported as the ones that led to the best results, and LANDW [18] a simultaneous projection method. For the LANDW method we used the relaxation parameter $\gamma = 2/L$, where L stands for an estimation of the maximum eigenvalue of $A^T A$ as given in [3].

The above mentioned algorithms converge to the minimum norm solution of the least squares problem if $x^0 \in R(A^T)$.

In [20] the authors reported comparisons with KR (Kaczmarz with relaxation parameters) and CEG [5], showing that KERP was the most efficient algorithm for several of the test problems which will be used here. In [23] we have also reported comparisons with ART(underrelaxed) [6, 16], CAV [8], LANDW and KE [19], showing that IOP was the most efficient algorithm for the test problems used for the comparison. Due to that reason, we compare KERP with our algorithm EIOP for rank-deficient problems.

All methods were implemented sequentially, and the experiences were run on a PC AMD Sempron 2.6, with 256 MB RAM.

In the implementation of EIOP we consider the parameter $\gamma = 10^{-2}$ in the initial iteration, then $\gamma = 10^{-1}$.

5.1. **Test problems.** The problems used for these numerical experiences are some from the RRA (real, rectangular, assembled) part of Harwell-Boeing Collection. Those least squares problems are from the set LSQ. In particular we use four matrices, such that the second and fourth matrix have the same pattern as the first and third respectively but are much more ill-conditioned. The matrices in this set are: WELL1033 and ILLC1033(real unsymmetric, 1033 by 320, 4732 entries), WELL1850 and ILLC1850 (real unsymmetric, 1850 by 712, 8758 entries). Also, aiming at testing problems with larger dimensions, we tested randomly generated dense matrices using DQRT15(LAPACK) which, using the parameter RKSEL = 2, generates a rank deficient matrix A(mxn) such that m is the number of rows and n is the number of columns of A, and rank $= \frac{3}{4}\min(m, n)$, whose dimensions appear in Table 2.

Other systems arise from the two image reconstruction problems used by Popa and Zdunek in [20]. They simulate real objects in electro-magnetic geotomography, leading to problems whose data comes from projections made with a limited angular range. Those problems are modeled by means of a system $Ax = b$, where b_i is the attenuation of the electro-magnetic field along the i-th ray, and each a_{ij} element of A represents the contribution of the j-th pixel, in relation to the i-th ray, to the attenuation b_i. Those problems lead to inconsistent systems, and the corresponding matrix has deficient rank due to the angle limitations of the projections. The first model ($A1$ matrix), whose original image is given in Figure 2 (left), is associated to an area of $12m \times 12m$, in a square of 12×12 pixels, the total number of rays being 144. The second model ($A2$ matrix), whose original image is presented in Figure 5 (left), has an area of $30m \times 30m$, represented in a square of 30×30 pixels, using 900 rays. The properties of these matrices are showed in Table 1.

For $A1$ and $A2$ we analyze the results with different systems $Ax = b + \delta b$, arising from simulating noisy perturbations of the right hand side $b = Ax^{exact}$. The problems here analyzed are exactly those of [20]. Starting from the knowledge of $b = Ax^{exact}$, a perturbation δb is defined satisfying $\|\delta b\|/\|b\| \approx 5.5\%$. Since

Properties	$A1$	$A2$
$m \times n$	144×144	900×900
Rank	125	805
Cond(A)	$9.39\ 10^4$	$2.15\ 10^7$
Sparsity	90.1%	95%
x^{exact}(image)	12×12 (pixels)	30×30 (pixels)

TABLE 1. Properties of $A1$ and $A2$

$\delta b = \delta b_A + \delta b_{A^\perp}$, where $\delta b_A \in R(A)$ and $\delta b_{A^\perp} \in R(A)^\perp$, the following cases are analyzed:

- Case (a): δb belonging to $R(A)^\perp$, that is $\|\delta b_A\| = 0$.
- Case (b): δb, satisfying $\|\delta b_A\| = \|\delta b_{A^\perp}\|$.

Those perturbations are applied to each problem according to:

- $A1$: (a) $\|\delta b_{A1}\| = 0$ and $\|\delta b_{A1^\perp}\| = 2.4874$; (b) $\|\delta b_{A1}\| = \|\delta b_{A1^\perp}\| = 1.76$
- $A2$: (a) $\|\delta b_{A2}\| = 0$ and $\|\delta b_{A2^\perp}\| = 15.9913$; (b) $\|\delta b_{A2}\| = \|\delta b_{A2^\perp}\| = 11.3076$.

Perturbations for both problems were computed using a standard procedure in MATLAB 5.3.

5.2. **Numerical results.** In this part of the numerical experiments we have considered in the implementation of EIOP the matrix $D_m = I_m$.

The problems used for these experiments are those described in the previous section, also adding the problems $A1$ and $A2$, labeled as case(c), when we consider solving the original consistent problem $Ax = b$, being $b = Ax^{exact}$ without perturbations. The minimum norm solution differs from x^{exact}, as can be seen in Figure 2(right) and Figure 5(right). The minimal 2-norm solution for both problems has been computed using a standard procedure in MATLAB 5.3.

First, we compare the algorithms in regard to the final residual corresponding to the satisfaction of the convergence criterion. According to the theoretical properties the three algorithms should tend to the same residual $\|b_{A^\perp}\|$.

The stopping condition for the three algorithms :
If $|\ \|r^{k+1}\| - \|r^k\|\ | < \epsilon \max(\|r^0\|, 1)$, with $\epsilon = 10^{-5}, 10^{-6}$ and 10^{-7}, aiming at analyzing the convergence rate. This choice was based on the fact all algorithms here analyzed converge to the minimum norm solution of the least squares problem. The convergence criterion allows to terminate the iterations when decreasing stagnates.

In Figure 1, we compare the performance of the methods in relation to the final residual obtained for each problem when the convergence criterion is met for the different values of the parameter ϵ. We analyze the performance data using profiles of Dolan and Moré, as described in [11]. Given the set of problems P and the set S of algorithms being analyzed, we compare the performance on problem p by a particular algorithm s with the best performance by any solver on this problem. Denoting by $R_{p,s}$ the residual obtained when solving problem $p \in P$ by the method $s \in S$, we define the performance ratio:

$$r_{p,s} = \frac{R_{p,s}}{\min_s\{R_{p,s} : s \in S\}}.$$

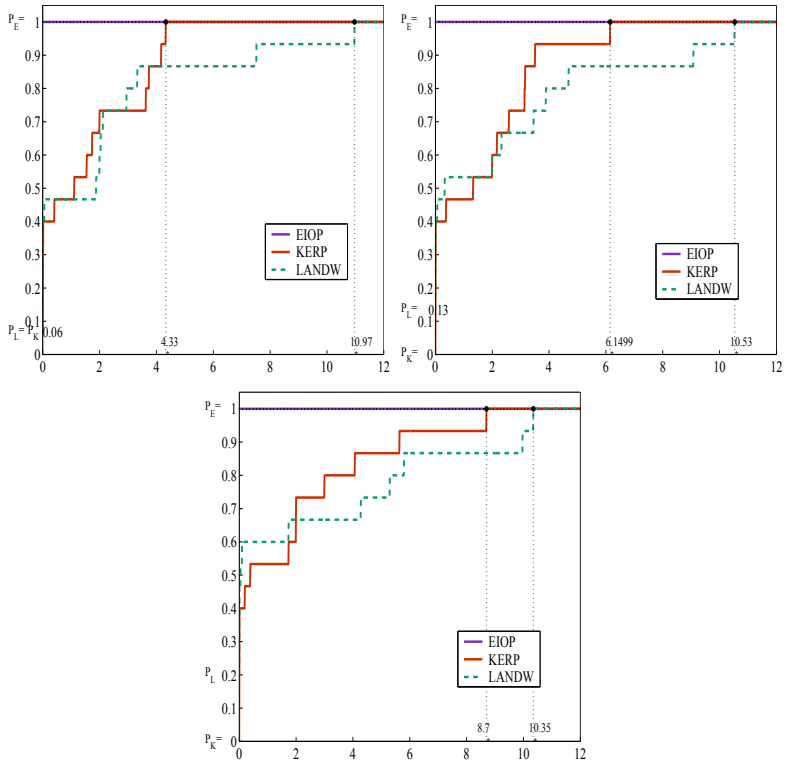

FIGURE 1. Performance profile in a scale log_2: $\epsilon = 10^{-5}$(top left), 10^{-6}(top right), 10^{-7}(bottom)

We also define the fraction $P_s(\tau) = \frac{1}{np} size\{p \in P : r_{p,s} \leq \tau\}$, where np is the number of solved problems.

In our drawings, since $r_{p,s}$ is large for several problems, we used a logarithmic scale in base 2 in the x-axis, as recommended in [11]. Thus, we draw $P_s(\tau) = \frac{1}{np} size\{p \in P : log_2(r_{p,s}) \leq \tau\}$, with $\tau \in [0, log_2(r_M)]$, where $r_M > 0$ is such that $r_{p,s} \leq r_M$, for all p and s.

In a performance profile plot, the top curve represents the most efficient method within a factor τ of the best measure. The percentage of the test problems for which a given method is best in regard to the performance criterion being studied is given on the left axis of the plot. In the drawings we pointed out the percentages corresponding to each algorithm by P_E for EIOP, P_K for KERP and P_L for LANDW. It is necessary to point out that when two different methods coincide with the best result, both receive the corresponding mark. This means that the sum of the successful percentages may exceed 100%.

As it can be seen in the plots of Figure 1 in most of the problems the final residual given by KERP and LANDW for the three different tolerances are significantly greater than those of EIOP. Due to that reason, in Table 2 we compare the number of iterations and the CPU time required by each algorithm to reach the residual obtained by EIOP with the tolerance $\epsilon = 10^{-6}$.

The dimensions of the test problems are shown using m for the number of rows, n for the number of columns. We show for each algorithm the number of iterations(**Iter**)required for obtaining a residual less or equal than $R_E(p)$, the value obtained by EIOP for each problem p, when using $\epsilon = 10^{-6}$ for the stopping criterion. We also give, the corresponding **CPU** time in seconds. In particular, for EIOP we report the number of inner iterations.

The starting point always was $x^0 = 0$.

A(mxn)	$R_E(p)$	CPU(sec.)/Iter		
		EIOP	KERP	LANDW
$A1(a)$(144x144)	0.70493	0.01/81	0.08/165	0.02/147
$A1(b)$(144x144)	0.70892	0.02/100	0.06/161	0.02/144
$A1$(c)(144x144)	4.941d-3	0.08/638	0.34/884	0.09/854
$A2(a)$(900x900)	2.95458	0.14/63	0.50 /81	0.33/157
$A2(b)$(900x900)	2.93782	0.20/89	0.51/88	0.33/158
$A2(c)$(900x900)	1.108d-2	0.97/326	2.22 /360	1.48/715
Rand(40x20)	8.166d-5	0.0001/48	0.002/166	0.002 /224
Rand(100x80)	1.57866	0.01/18	0.03/21	0.02/43
Rand(500x300)	6.98662	0.11/17	0.39 /24	0.25 /38
Rand(3000x2000)	2.484d-4	15.6 /55	164.2 /169	2554.0/9809
Rand(4000x2000)	9.013d-5	20.1 / 56	602.8 /102	4297.0/12454
Illc(1033x322)	15948.06	0.12/286	4.44/5005	27.0/89050
Illc(1850x712)	2.53336	13.8/17696	686.0/404832	3688.0/4235678
Welc(1033x322)	1.89446	0.61/1479	33.4 / 36167	509.6/1741562
Welc(1850x712)	2.62300	1.96/2519	25.8 / 14654	1240.0 /3181617

TABLE 2.

It is necessary to point out that each KERP iteration requires approximately the double of projections than an internal EIOP iteration. This can be seen in Table 2 where almost an identical number of iterations for both algorithms differ in practically the double of CPU time.

It follows from those results that the EIOP method is faster than the known algorithms, and is also able to reduce the residual more rapidly.

5.3. **Image reconstruction results.** We have made some experiences to illustrate the behavior of EIOP in the solution of image reconstruction problems, when data comes from projections made with a limited angular range, as in electro-magnetic geotomography [20]. With the purpose of displaying the quality of the reconstructed image we compared EIOP with those obtained with KERP. These experiences were made using two image models, "phantoms", provided by C. Popa and R. Zdunek, that are exactly those reported in their paper [20] and correspond to those mentioned before as $A1$ and $A2$, case(a) and (b).

In this part, the matrix D_m used in the implementation of EIOP was $D_m = diag(\|a_i\|^2)$, that was the one that gave the best performance in regard to the descent of the norm of the residual, among several alternatives.

We compare the performance of the algorithms, by a curve representing the distance of the obtained density with regard to the one of the true image, and also the quality of the reconstructed image by each algorithm.

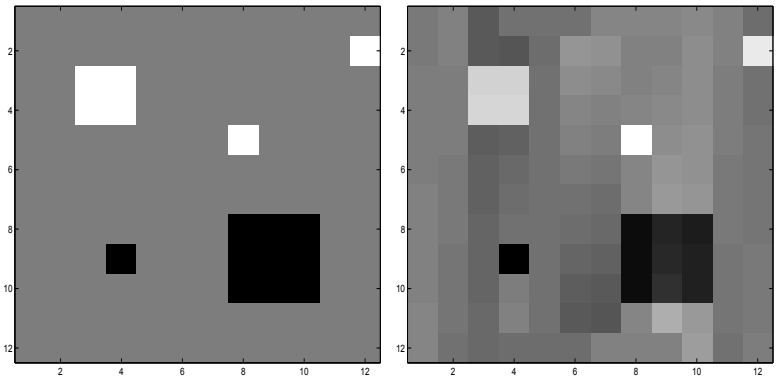

FIGURE 2. $A1$: Exact Image(left) Minimal Norm Solution(right)

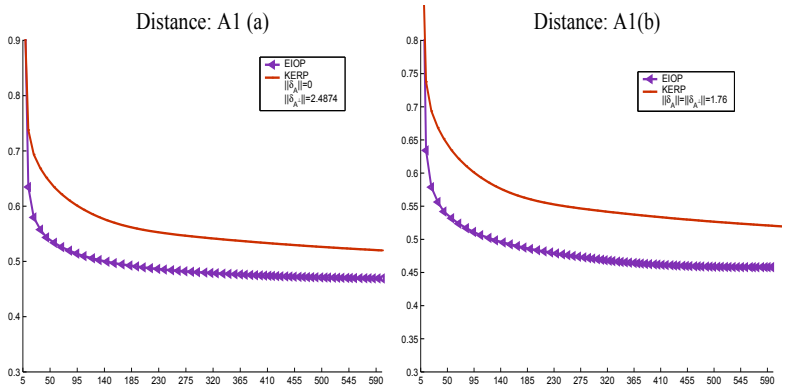

FIGURE 3. Distance: $A1$(a)(left), $A1$(b)(right)

The formula of *Distance* [7], between the solution x^k (k-th iteration) and the true image x^{exact}, is: $\frac{\|x^k - x^{exact}\|}{\sqrt{N}\sigma_{exact}}$, being $\sigma_{exact} = \|x^{exact} - \rho_{exact}\|$, where $\rho_{exact} = \frac{\sum_{j=1}^{N} |x_j^{exact}|}{N}$.

In Figure 3, we compare the performance of EIOP and KERP in regard to the distance of the reconstructed images for test problems $A1$ case(a) and case(b). In Figure 3(left), $A1$ case(a), we observe that EIOP gives a distance in the 50th iteration less than the one obtained by KERP in 500 iterations. This result is coherent with the ones of the previous subsection where we showed that EIOP reduces the residual much faster than KERP. Since the perturbation has $\delta b_A = 0$, both algorithms converge to the minimum norm solution of $A1x = b$, without perturbations.

For saving space we will only show the reconstructed images for case(b). In Figure 4 the reconstructed images corresponding to $A1$ case(b) are shown for KERP (top row) and EIOP (bottom row) respectively, at iterations 57, 156 and 251. It is necessary to point out that the number of iterations are the internal ones for EIOP, while for KERP are the number of performed global iterations. The criterion used for reporting the obtained images in the specified iterations was to choose those

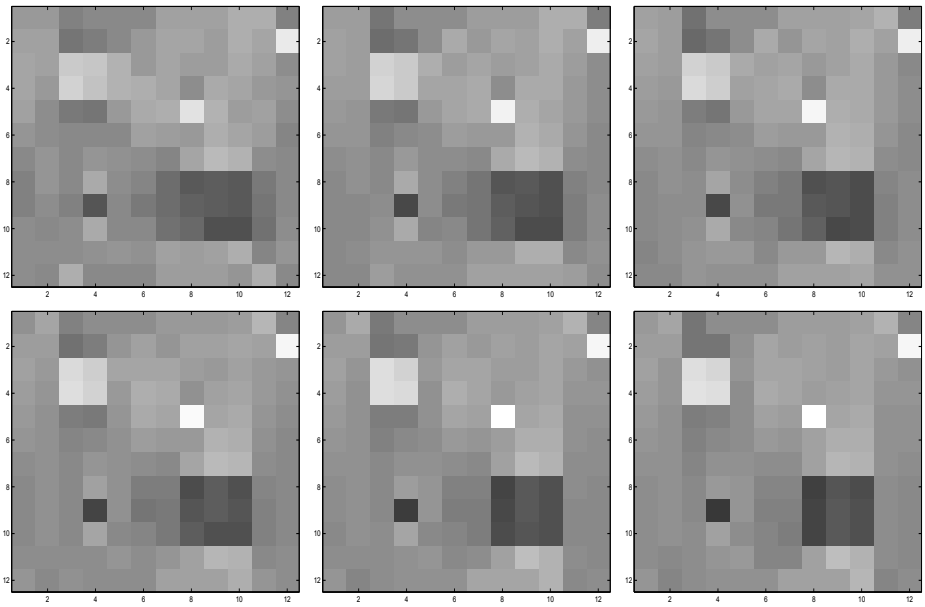

FIGURE 4. $A1$(b): KERP (top), EIOP (bottom), 57, 156, 251 iterations

closer to 50-150-250, as given in [20]. For case (b), the perturbation is of the sort $\|\delta b_A\| = \|\delta b_{A^\perp}\|$, and since both algorithms converge to the minimum norm solution, the term $\|\delta b_{A^\perp}\|$ has neither influence on the reconstructed images nor on the distance to the exact solution. However, $\|\delta b_A\| \neq 0$ is important. Figure 3 (right) shows the same behavior as before in regard to the distance to the exact solution. This is compatible with what shows Figure 4 where the comparison between the images of the case $A1(b)$ shows that KERP at iteration 156 is less smooth than the one given by EIOP at iteration 57. Also, at iteration 251 the image corresponding to EIOP is more homogeneous than the one of KERP, and is much more similar to the image appearing in Figure 2 (right). It is worthwhile to point out that EIOP is stable in regard to small perturbations, and obtains more rapidly better reconstructions and less distances to the true solution than KERP. In Figure 6 the performance of EIOP and KERP are compared in relation to the distance of the reconstructed images for $A2$ case(a)(left) and case(b)(right), respectively. Also, in Figure 7 we show the reconstructed images of problem $A2$ case(b) by the same algorithms corresponding to the iterations 57, 154 and 269, chosen as explained before.

As it can be seen in the curves and images, EIOP reaches in a faster way, approximately at the 70-th iteration, the image closest to the original for $A2$ problem, cases (a) and (b). Likewise EIOP obtains the minimum distance, and keeps it below the one corresponding to KERP, between the 50-th and the 500-th iterations. This is compatible with what can be seen in Figure 7, where the images reconstructed by EIOP at iterations 57 and 154 are sharper and with less artifacts than those given by KERP at iterations 154 and 269, respectively.

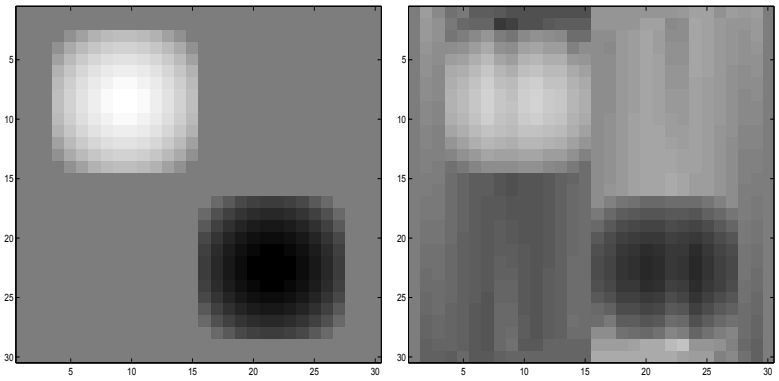

FIGURE 5. $A2$: Original Image(left) Minimal Norm Solution(right)

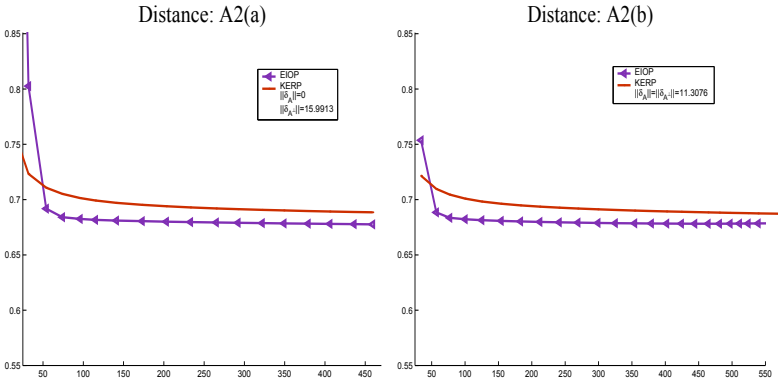

FIGURE 6. Distance: $A2$(a)(left), $A2$(b)(right)

Conclusions. The aim of this paper was to show that a version of IOP [23] for the rank-deficient case is also efficient. In that paper we have compared its performance with several algorithms, as ART (underrelaxed) which is one of the most important class of methods used for solving image reconstruction problems, and CAV [7], using test problems from SNARK [2], showing that is very efficient. In this paper the comparison is only made with KERP because the authors [20] said that it has a better performance than the underrelaxed ART. The numerical results given here demonstrate that EIOP outperforms KERP, both in the rate of convergence and the required CPU time. In the case of image reconstruction problems, EIOP obtains the closest image to the original one in much less CPU time than KERP.

In a future paper we will present a modification of the least squares model (1), used for image reconstruction. This is so because not always the minimum norm solution turns out to be the closest to the true image due to the underlying discretized model. Therefore, we are studying how to penalize the model (1) in order to match convergence with image quality.

Acknowledgements. We would like to thank C. Popa and R. Zdunek for having kindly provided their test problems used in [20].

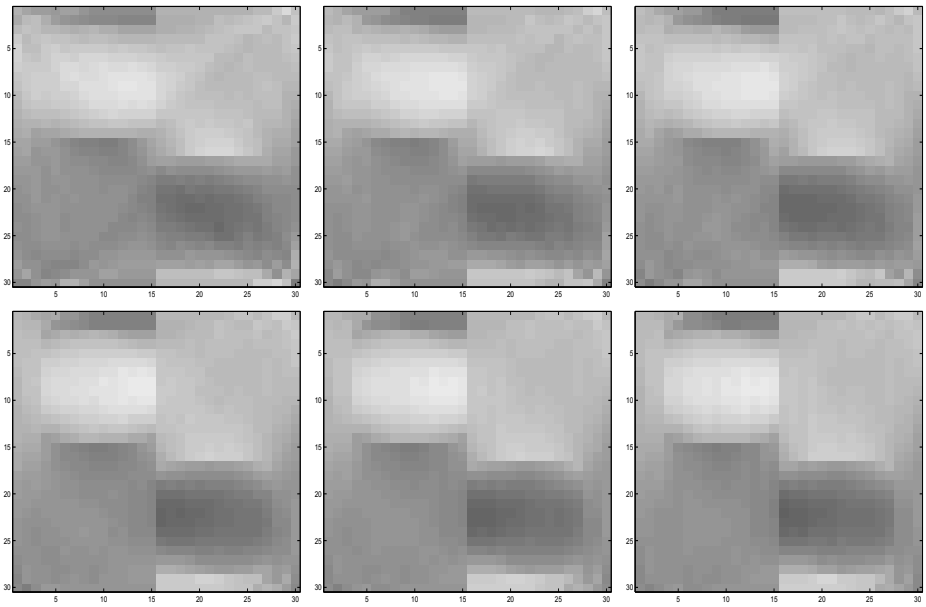

FIGURE 7. $A2$(b): KERP (top), EIOP (bottom), 57, 154, 269 iterations

REFERENCES

[1] W. Briec and B. Solonandrasana, *Some remarks on a succesive projection sequence*, Journal of Industrial and Management Optimization, **2** (2006), 451–466.

[2] J. A. Browne, G. T. Herman and D. Odhner, "SNARK93: A Programming System for Image Reconstruction from Projections," Department of Radiology, University of Pennsylvania, Medical Image Processing Group, Technical Report MIPG198, 1993.

[3] C. Byrne,*Iterative oblique projection onto convex sets and the split feasibility problem*, Inverse Problems, **18** (2002), 441–453.

[4] C. Byrne, and Y. Censor, *Proximity function minimization using multiple bregman projections with applications to split feasibility and Kullback-Leibler distance minimization*, Annals of Operations Research, **105** (2001), 77–98.

[5] Y. Censor, P. B. Eggermont and D. Gordon, *Strong underrelaxation in Kaczmarz's method for inconsistent systems*, Numer. Math., **41** (1983), 83–92.

[6] Y. Censor and S. Zenios, "Parallel Optimization: Theory and Applications," Oxford University Press, New York, 1997.

[7] Y. Censor, D. Gordon and R. Gordon, *Component averaging: An efficient iterative parallel algorithm for large and sparse unstructured problems*, Parallel Computing, **27** (2001), 777–808.

[8] Y. Censor and T. Elfving, *Block-iterative algorithms with diagonally scaled oblique projections for the linear feasibility problem*, SIAM J. Matrix Anal. and Applicat., **24** (2002), 40–58.

[9] MR1272203 P. Combettes and H. Puh, *Iterations of parallel convex projections in Hilbert spaces*, Numer. Funct. Anal. Optim. **15** (1994), 225–243.

[10] I. Csiszár and G. Tusnády, *Information geometry and alternating minimization procedures*, Statistics and Decisions, Supplement, **1** (1984), 205–237.

[11] E. D. Dolan and J. J. Moré, *Benchmarking optimization software with performance profiles*, Mathematical Programming, **91** (2002), 201–213.

[12] N. Echebest, M. T. Guardarucci, H. D. Scolnik and M. C. Vacchino, *An accelerated iterative method with diagonally scaled oblique projections for solving linear feasibility problems*, Annals of Operations Research, **138** (2005), 235–257.

[13] U. M. García Palomares, *Parallel projected aggregation methods for solving the convex feasibility problem*, SIAM J. Optim., **3** (1993), 882–900.

[14] G. T. Herman and L. B. Meyer, *Algebraic reconstruction techniques can be made computationally efficient*,IEEE Trans. Medical Imaging, **12** (1993), 600–609.
[15] A.S. Householder and F. L. Bauer, *On certain iterative methods for solving linear systems*, Numer. Math., **2** (1960), 55–59.
[16] S. Kaczmarz, *Angenäherte Auflösung von systemen linearer Gleichungen*, Bull. Intern. Acad. Polonaise Sci. Lett., **35** (1937), 355–357.
[17] M. Jiang and G. Wang, *Convergence studies on iterative algorithms for image reconstruction*, IEEE Transactions on Medical Imaging, **22** (2003), 569–579.
[18] (13,247c) L. Landweber, *An iteration formula for Fredholm integral equations of the first kind*, Amer. J. Math., **73** (1951), 615–624.
[19] C. Popa, *Extensions of Block-Projections methods with relaxation parameters to inconsistent and rank-deficient least-squares problems*, BIT, **38** (1998), 151–176.
[20] C. Popa and R. Zdunek, *Kaczmarz extended algorithm for tomographic image reconstruction from limited-data*, Mathematics and Computers in Simulation, **65** (2004), 579–598.
[21] H. D. Scolnik, N. Echebest, M. T. Guardarucci and M. C. Vacchino, *A class of optimized row projection methods for solving large non-symmetric linear systems*, Applied Numerical Mathematics, **41** (2002), 499–513.
[22] H. D. Scolnik, N. Echebest, M. T. Guardarucci and M. C. Vacchino, *Acceleration scheme for parallel projected aggregation methods for solving large linear systems*, Annals of Operations Research, **117** (2002), 95–115.
[23] H. D. Scolnik, N. Echebest, M. T. Guardarucci and M. C. Vacchino, *Incomplete oblique projections for solving large inconsistent linear systems*, Mathematical Programming , Ser. B, **111** (2008), 273–300.

Received April 2007; 1st revision January 2008; 2nd revision February 2009.

E-mail address: hscolnik@gmail.com
E-mail address: opti@mate.unlp.edu.ar
E-mail address: marite@mate.unlp.edu.ar